Journal of Materials Chemistry C

PAPER

View Article Online
View Journal | View Issue

Cite this: J. Mater. Chem. C, 2014, 2, 9182

Efficient energy transfer from ZnO to Nd^{3+} ions in Nd-doped ZnO films deposited by magnetron reactive sputtering†

Matteo Balestrieri,*[a] Silviu Colis,*[a] Mathieu Gallart,[a] Gérald Ferblantier,[b] Dominique Muller,[b] Pierre Gilliot,[a] Paul Bazylewski,[c] Gap Soo Chang,[c] Abdelillah Slaoui[b] and Aziz Dinia[a]

In this paper, a detailed study of the luminescent properties of Nd^{3+} ions in sputtered ZnO thin films is reported for the first time. Experimental evidence is provided showing that Nd is inserted and optically active in the ZnO matrix. Despite the small amount (<2%) of rare earth in these thin ZnO films, intense luminescence signals have been collected, indicating efficient infrared emission of Nd^{3+} in ZnO. Direct excitation of Nd^{3+} ions in the ZnO matrix was possible, suggesting that most of the Nd atoms are in the 3+ form at all deposition temperatures. Moreover, intense Nd^{3+} emission has been recorded also when the host was excited, indicating that an efficient energy transfer occurs from ZnO to Nd ions. Both the transfer efficiency and the Nd^{3+} concentration seem to depend on the deposition temperature. In particular, indirect excitation of the sample deposited at 400 °C generates a richer emission pattern compared to lower temperatures. The careful analysis of the luminescence data indicated that the new pattern comes from Nd sites that cannot be efficiently directly excited, but that are characterized by intense emission under indirect excitation of the host. The possible transfer mechanisms leading to this behavior will be outlined.

Received 12th May 2014
Accepted 3rd September 2014

DOI: 10.1039/c4tc00980k

www.rsc.org/MaterialsC

Introduction

In the past decades, rare earth (RE)-doped phosphors have found applications in many fields of technology. Pioneering work has led to the development of semiconductor lasers and optical fibers, mainly based on the near infrared (NIR) emission of Nd, Er, Yb and Tb. At a later stage, the development of flat panel displays boosted the research on RE ions with visible-range emission such as Eu, Pr, Tb, Er, and Sm.[1–3] At the same time, the concepts of wavelength conversion and photon cutting have further stimulated the research and opened the way to new applications of RE-activated phosphors. In particular, the photon management properties of RE ions seem to be very promising for reducing the optical losses of solar cells.[4,5] By adapting the incident solar spectrum to a specific single junction solar cell, the photovoltaic conversion efficiency can be enhanced. One of the advantages of this approach is that higher efficiency can be reached without changing the solar cell structure. For this purpose, the RE ions must be inserted into one of the transparent windows most typically used in standard solar cells (encapsulant, transparent conductive oxides (TCOs)). However, due to the small absorption cross-section of RE ions, energy transfer from an absorbing host might be the only way to obtain reasonable quantum yields. Wide band gap semiconductors such as ZnO,[6,7] SnO_2,[8] and TiO_2 (ref. 9) provide the necessary absorption in the UV region and are therefore promising host materials.

Compared to other TCOs, ZnO combines several advantages such as high exciton binding energy (60 meV (ref. 10)), good n-type conductivity based on oxygen vacancies, low cost and low toxicity. Moreover, the direct-allowed band gap of 3.37 eV provides a strong absorption cross-section over a wide region of the solar spectrum.

In the past few years, efficient doping of ZnO thin films with several REs has been achieved by means of physical deposition techniques.[7,11–13]

The selection of the appropriate host for each RE is a non-trivial matter and cannot be done *a priori*. Due to the large ionic radius of REs, insertion of these ions into a specific host material can be quite a difficult task. For this reason, physical deposition techniques like sputtering should provide better dopant insertion compared to chemical approaches. In addition, optical activation of the ions is necessary.

[a]Institut de Physique et Chimie des Matériaux de Strasbourg, Université de Strasbourg, CNRS UMR 7504, 23 rue du Loess, B.P. 43, F-67034 Strasbourg Cedex 2, France. E-mail: m_balestrieri@libero.it; colis@ipcms.u-strasbg.fr; Tel: +33 3 88 10 71 29

[b]Laboratoire ICube, Université de Strasbourg, CNRS UMR 7357, 23 rue du Loess, B.P. 20, F-67037 Strasbourg Cedex 2, France

[c]Department of Physics and Engineering Physics, University of Saskatchewan, 116 Science Place, Saskatoon, SK S7N 5E2, Canada

† Electronic supplementary information (ESI) available. See DOI: 10.1039/c4tc00980k

Since the crystal field is responsible for the wavefunction mixing necessary to overcome the forbidden nature of the inter-4f shell transitions, the strength and the specific (non-spherical) symmetry of the crystal field at the insertion site are very important host-dependent parameters. Moreover, other host properties such as the band gap and the lattice defects can influence the emission efficiency.

Three kinds of optical losses affect single junction solar cells, namely thermalization, transparency, and low blue response. In the frame of photon management, the three processes that can recover these losses are down-conversion (DC), up-conversion (UC) and down-shifting (DS), respectively.[4] The specific loss can be targeted by choosing the appropriate host and RE.

Doping ZnO with Nd ions is particularly interesting due to the rich level structure of Nd^{3+}, which is potentially suited for recovering all three optical losses. Although some work exists on Nd-doped ZnO thin films,[11,14–16] no extensive investigation of the luminescent properties has been performed yet. In this paper, a detailed study of the luminescent properties of Nd^{3+} ions in ZnO thin films is reported for the first time.

Experimental

Nd-doped ZnO thin films were deposited on p-type Si(100) by radio frequency (RF) magnetron reactive sputtering using an Orion 3 device from AJA International Co. Doping was carried out by placing several pure RE metal discs on the surface of pure zinc targets (sputtering with substrate-on-top configuration and one target per RE). Two different Nd concentrations have been investigated: 1 at% and 1.6 at% with respect to the Zn content. The higher concentration produces stronger signals, but similar results. Therefore, most of the results will be presented for this concentration.

Oxygen was added into the sputtering chamber to form the final ZnO:Nd film. The Ar/O_2 gas flow ratio was fixed at a value of 4. The RF power and deposition pressure were optimized to 50 W and 3.4 mTorr, respectively. The substrate to target distance was kept constant at about 12 cm. The deposition time has been adjusted in order to have the desired film thickness of 100 nm.

Since the deposition temperature is known to be a key parameter for dopant insertion and activation, it was varied between 15 °C (environment of the substrate holder cooled with water) and 500 °C.

The structural properties of the films were analyzed in the 20–130° 2θ range by means of a Rigaku SmartLab® X-ray diffractometer equipped with a monochromatic source (Ge(220)x2) delivering a Cu Kα1 incident beam (45 kV, 200 mA, $\lambda = 0.154056$ nm). The crystallite size and the lattice parameter along the growth direction have been calculated using Bragg's law and Scherrer's formula.

The film thickness and optical constants were measured with a HORIBA UviselTM Lt M200 FGMS (210–880 nm) spectroscopic ellipsometer.

Photoluminescence (PL) measurements were performed in order to obtain insight into the insertion and activation of Nd in ZnO as well as on the electronic level structure of Nd^{3+} ions and on the energy transfer from ZnO to Nd ions. Excitation was provided both by the 325 nm line of a He–Cd laser and a broad-spectrum Energetiq® EQ-99FC laser-driven light source (LDLS™) equipped with a monochromator. The signals were recorded by means of a liquid N_2-cooled CCD camera and an InGaAs detector. Low-temperature PL was measured close to the temperature of liquid He using an Oxford MG11 cryostat. Particular attention was paid to eliminate parasitic luminescence coming from the environment and from the excitation by using a set of filters. The spectra presented here have been corrected for the filter and lamp emission, as well as for the detector response.

Element-specific near edge X-ray absorption fine structure (NEXAFS) spectroscopy was employed to investigate the Nd valence in Nd-doped ZnO films. Spectroscopic measurements at the Nd $M_{4,5}$ edge were performed at the Resonant Elastic-Inelastic X-ray Scattering (REIXS) beamline of the Canadian Light Source. The Nd $M_{4,5}$ NEXAFS spectra were obtained in total electron yield (TEY) mode at a 45° angle of incidence and were normalized to the incoming photon flux recorded by an Au mesh and to a constant background at 980 eV.

Rutherford backscattering spectroscopy (RBS) measurements were carried out at room temperature using a $^4He^{2+}$ particle beam with an energy of 2 MeV. A Van de Graaff particle accelerator provided the necessary 4 MV accelerating voltage.

Results and discussion

The structural and morphological investigations showed that highly oriented and uniform ZnO:Nd thin films have been obtained. RBS measurements indicated a uniform Nd concentration along the growth direction (see Fig. S1 of the ESI†), which is independent of the deposition temperature. Fig. 1 shows that all films have the expected wurtzite structure with a strong texture along the [002] direction. Neither secondary phase nor Nd oxide peaks have been observed in the detection limit of the X-ray diffraction (XRD) technique. The crystallite

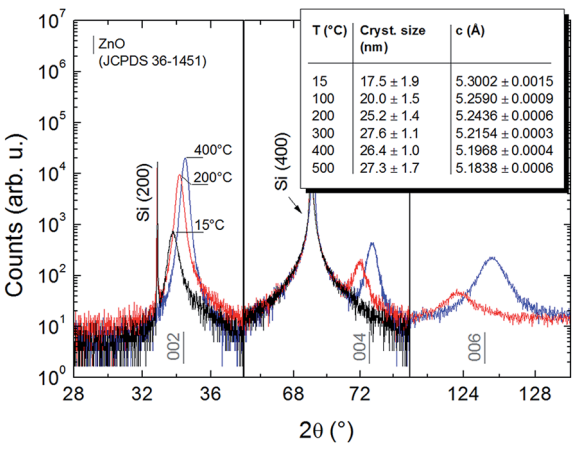

Fig. 1 X-ray diffractograms of the ZnO:Nd thin film deposited at different temperatures. The inset shows the crystallite size and the lattice parameter along the growth direction for all deposition temperatures. No (006) peak has been observed for the sample grown at 15 °C and the relative data have been omitted for clarity.

size and the lattice parameter along the growth direction are reported in the inset table. The use of high deposition temperatures leads to higher crystalline quality. The compressive stress induced by the large Nd ions in the substitutional position and other lattice defects is reduced, as indicated by the decrease of the lattice parameter. Above 400 °C, the lattice parameter is smaller than the bulk value (5.2066 Å), suggesting the introduction of a small tensile stress. On the other hand, the crystallite size increases up to 200 °C and stabilizes around 27 nm for higher temperatures.

Fig. 2 shows the near infra-red (NIR) emission spectra under 325 nm laser excitation of ZnO:Nd (1.6%) films deposited at different deposition temperatures. The main group of emission lines is centered at 920 nm and is usually attributed to the $^4F_{3/2} \rightarrow {}^4I_{9/2}$ transitions of Nd^{3+}.[8,17] The second, less intense group appears around 820 nm and can be attributed to the $^4F_{5/2} \rightarrow {}^4I_{9/2}$ transitions. No emission related to Nd^{3+} has been detected below 700 nm. One explanation could be that energy transfer from ZnO only excites the lowest levels of Nd^{3+}. Alternatively, given the large number of excited states above the $^4F_{3/2}$ level and the quite large phonon energy of ZnO, non-radiative relaxation processes might occur when the electron is excited to higher states. These spectra, recorded by the CCD camera, cover the spectral range useful for solar cell applications. However, lower infrared emission of ZnO:Nd films could be useful for other optoelectronic devices. A more extended range will be studied further below.

It is interesting to note in Fig. 2 that the shape and intensity of the emission spectra do not present major changes up to a deposition temperature of 300 °C (except for a slight decrease of the intensity). At 400 °C, the overall emission increases and some of the peaks become particularly strong. A similar pattern has been obtained by Liu *et al.*[17] for Nd-doped ZnO nanocrystals annealed at 400 °C. Although not all the individual peaks are well defined, it is clear that these bands contain more than five peaks expected for the crystal field splitting of the $^4I_{9/2}$ level. The position of the observed peaks that could be distinguished is also indicated in Fig. 2. In ref. 17, the authors attributed the rich pattern to several active sites for Nd^{3+} in the ZnO lattice. New evidence presented in this paper allows deeper insight into the different active sites.

First of all, a closer look at Fig. 2 shows that practically all the peaks that become so intense above 400 °C are already there for lower temperatures, but very small. This means that either high temperatures promote the creation of this second Nd site or the energy transfer to this site is improved.

The smooth variations of the lattice parameter and the crystallite size with the deposition temperature make it difficult to ascribe the abrupt increase in the PL to the structural properties of the films.

Additional information can be obtained by studying the excitation spectrum of the PL emission, *i.e.* by looking at the evolution of the PL emission intensity when the excitation wavelength is varied.

Wide range (300–800 nm) PL excitation (PLE) spectra of ZnO:Nd emission were recorded at room temperature. For simplicity, only the PLE of selected emission lines is reported in this paper. The PLE of the most intense emission peak, situated at 902 nm, is reported in Fig. 3 for three deposition temperatures. The smooth excitation spectrum below 400 nm follows the typical absorption edge of ZnO (ref. 7) and gives experimental proof that energy transfer occurs from the host to Nd ions.

This means that excitons and electrons, while recombining across the gap or through some lattice defects in the neighborhood of Nd ions, can transfer some energy to 4f electrons of Nd^{3+}, which are then promoted to an excited state. In this case, the highest accessible excited state of Nd^{3+} is limited by the band gap value or the amplitude of the defect-related transition.

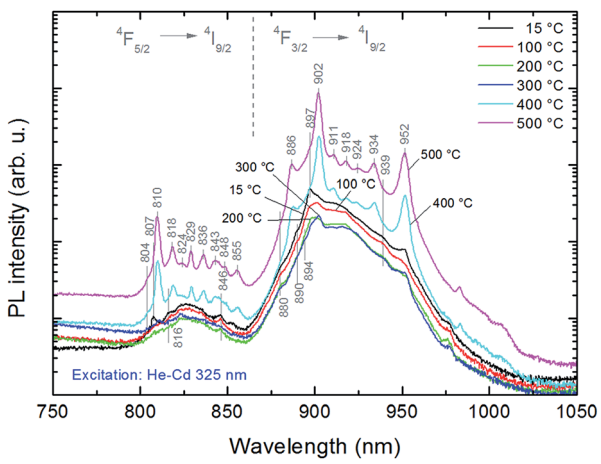

Fig. 2 NIR PL emission spectra of ZnO:Nd thin films deposited at different temperatures and excited by the 325 nm line of a He–Cd laser. Two bands associated with radiative transitions between the $^4F_{5/2}$ and $^4F_{3/2}$ excited states to the $^4I_{9/2}$ fundamental state multiplet can be distinguished. The approximate position of the individual lines is also indicated.

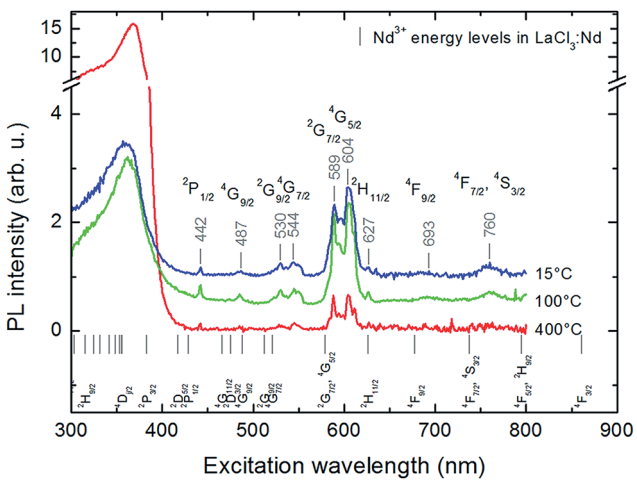

Fig. 3 Room temperature PL excitation spectra of the 902 nm emission line of ZnO:Nd thin films deposited at different temperatures. The electronic level configuration of Nd^{3+} in $LaCl_3$:Nd crystals is reported for comparison.[18]

It is difficult to quantify the real efficiency of this process using PLE, since only radiative recombination is detected.

Fig. 3 also shows that Nd^{3+} emission can be obtained even by exciting below the band gap value of ZnO (*i.e.* above 400 nm). In this case, the excitation is distributed in several relatively narrow peaks centered at 442, 487, 530, 544, 589, 604, 627, 693 and 760 nm. Comparison with the electronic level configuration of Nd^{3+} in $LaCl_3$:Nd crystals indicates that these peaks correspond to direct excitation of Nd^{3+}. It is interesting to note that almost all levels of Nd^{3+} in ZnO are red-shifted with respect to those in $LaCl_3$ and present a stronger Stark-splitting, evidencing the strong crystal field experienced by Nd^{3+} in the ZnO lattice. The peak positions are very close to those of Nd^{3+} in ZnO nanocrystals.[17]

The spectra in Fig. 3 show that the energy transfer from the host is efficient enough for the emission to be higher than that resulting from direct excitation. Moreover, the wide absorption region of ZnO increases the advantage of indirect excitation.

Compared to the samples prepared at lower temperatures, the excitation efficiency of the sample deposited at 400 °C appears to be different. In particular, the emission intensity is higher under indirect excitation and lower under direct excitation.

Fig. 4 illustrates what happens to the whole $^4F_{3/2} \rightarrow {}^4I_{9/2}$ emission band. Here, the emission of a sample deposited at 100 °C is compared with that of the sample deposited at 400 °C in the case of direct and indirect excitation. In the case of the sample deposited at low temperature, the shape of the PL presents only small changes between direct and indirect excitation. The intensity of the two emissions is comparable, indicating that the limiting factor is probably the emission yield from this active site, rather than the transfer efficiency. It is interesting to notice that in the case of the sample deposited at 400 °C, the emission spectrum under direct excitation is exactly the same as that of the sample deposited at low temperature, but with lower intensity. On the other hand, the spectrum under indirect excitation reproduces the results of Fig. 2. This means that the Nd site activated at high temperature cannot be efficiently directly excited. Another interesting result is that direct excitation of higher excited states produces the same emission bands in the infrared region as indirect excitation. This supports the hypothesis that non-radiative relaxation occurs until the electron reaches the $^4F_{3/2}$ state.

In order to exclude the influence of a different absorption cross-section of ZnO, the absorption edge is reported in Fig. S2 of the ESI.† At the excitation wavelength, corresponding to 3.8 eV, the differences in the absorption coefficient are relatively small compared to the differences in PL. Moreover, the absorption increases continuously with the deposition temperature. A variation of the band gap is also observed. More information on this point will be given below, when the transfer mechanisms will be discussed.

Although a complete deconvolution of the bands is quite a difficult task, more information can be obtained by recording the emission at a very low temperature, where the contribution of phonons is reduced.

Fig. 5 reports the emission spectra recorded at RT and 15 K for the samples deposited at 15 °C and 400 °C. Indeed, many transitions are suppressed at such a low temperature. In particular, the whole $^4F_{5/2} \rightarrow {}^4I_{9/2}$ emission band disappears. This fact can be explained by assuming that these transitions can only occur following a phonon-assisted process. The fact that the energy separating the $^4F_{5/2}$ level from the $^4F_{3/2}$ level is approximately the energy of two longitudinal optical phonons in ZnO (72 meV (ref. 19)) supports this hypothesis.

Additional information can be obtained if the detection range is extended in the infrared region, where the other two main emission lines of Nd^{3+} are expected.[8,20] These lines are commonly attributed to the $^4F_{3/2} \rightarrow {}^4I_{11/2}$ and $^4F_{3/2} \rightarrow {}^4I_{13/2}$ transitions of Nd^{3+}.

In Fig. 6, wide-range low-temperature emission spectra of samples deposited at 15 °C and 400 °C under laser excitation are reported. The three line groups commonly attributed to the

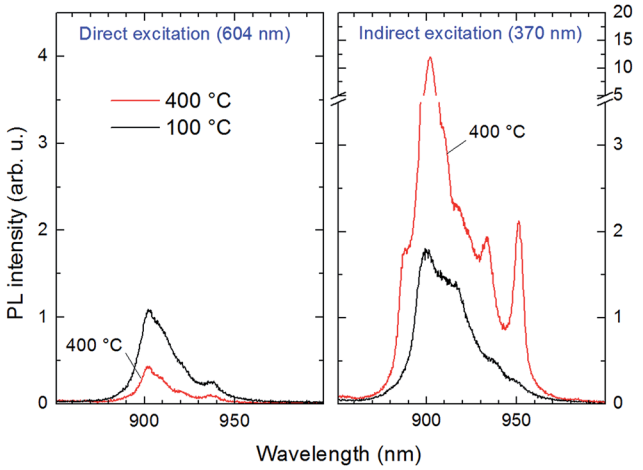

Fig. 4 Room temperature PL emission under direct (604 nm) and indirect (370 nm) excitation for ZnO:Nd thin films deposited at 100 °C and 400 °C.

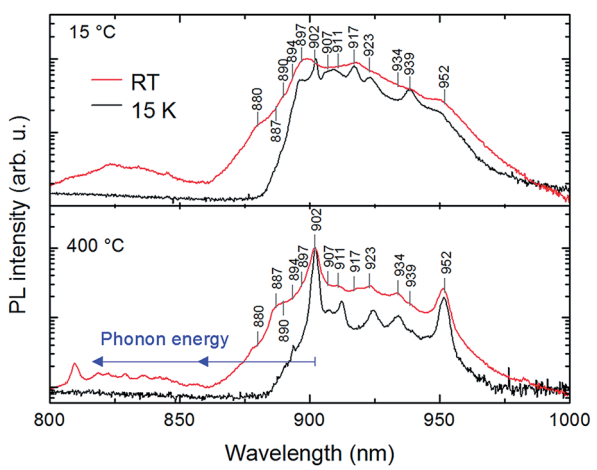

Fig. 5 Normalized emission spectra of the samples deposited at 15 °C and 400 °C following He–Cd laser excitation and recorded at RT and at 15 K.

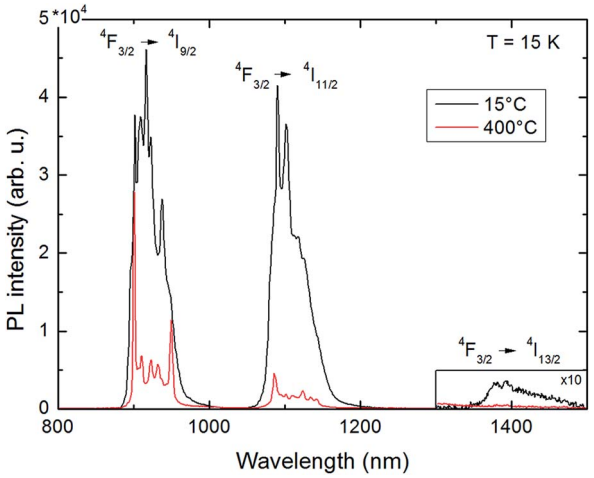

Fig. 6 Low temperature PL emission spectra of samples deposited at 15 °C and 400 °C under He–Cd (325 nm) laser excitation.

$^4F_{3/2} \rightarrow {}^4I_J$ transitions can be identified. However, these transitions alone cannot account for the rich pattern observed. In fact, even for the sample deposited at 15 °C, the simplest deconvolution of each group requires not less than 15 Gaussian peaks, which is more than twice the maximum multiplicity $(2J+1)/2$ of the ^4I_J levels after the degeneracy lift due to the Stark effect in the ZnO crystal field. The maximum multiplicity could be doubled due to the multiplicity of the $^4F_{3/2}$ level, but the position of the peaks is not compatible with this hypothesis.

This can indeed be interpreted as an indication that several active sites for Nd^{3+} exist in ZnO. However, due to the large superposition of the different emission patterns, the separation of the different contributions is a very difficult task even at such low temperatures.

Deeper insight into the energy level structure of Nd^{3+} and into the energy transfer from ZnO can be obtained by means of low temperature PLE measurements. The low temperature PL spectra under selected excitations are reported in the inset in Fig. 7 for the sample deposited at 15 °C. Under indirect excitation (360 nm), the spectrum presents a rich pattern of emission lines. Up to seven emission lines can be clearly distinguished, but not all seven can be directly excited at the same time. The peaks at 895 nm and 916 nm present a different excitation spectrum. The PLE spectra of the 895, 902 and 916 nm emission lines are presented in Fig. 7.

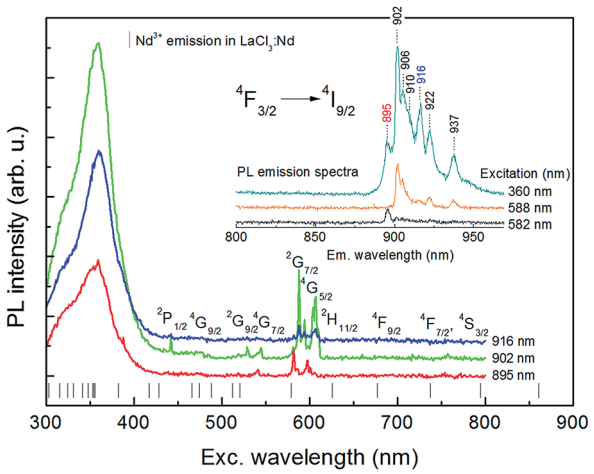

Fig. 7 Low temperature (3.2 K) PL excitation spectra of the emission lines at 985, 902 and 916 nm recorded on ZnO:Nd (1%) thin films deposited at 15 °C. Inset: low temperature PL emission spectrum of ZnO:Nd (1%) under different excitations.

The peak at 895 nm can also be induced by direct excitation, but from different Nd^{3+} levels. This suggests that it is not part of the $^4F_{3/2} \rightarrow {}^4I_{9/2}$ group. The fact that it can be observed following direct excitation of the $^4G_{5/2}$ and/or $^4G_{7/2}$ levels might suggest that this peak originates from a transition between an excited state situated between these levels and the $^4F_{3/2}$ level to one of the ^4I_J multiplets. The other intense emission peak can be found at 916 nm. It seems that this peak can be excited only indirectly, just as the intense peaks described above. The weak peaks in the excitation spectrum are probably derived from the convolution with the surrounding peaks. The origin of this peak is not clear yet.

The PLE spectrum of the 902 nm emission line clearly shows that some of the direct excitation peaks disappear at low temperatures (*e.g.* those at 487 and 760 nm). This might be due to a different crystal field sensed by the Nd ions at such a low temperature. Alternatively, it might indicate that phonons may play an important role in direct excitation.

Comparison of the PLE at 895 nm and 902 nm shows that the $^2G_{7/2}/^4G_{5/2}$ group splits into at least 9 lines, exceeding the maximum total multiplicity of these two levels. This is in contrast to the explanation given above for a different transition and supports the hypothesis of the third active site for Nd^{3+}.

At this point, it is important to understand why some emission lines should only be excited by energy transfer from the host.

In the case of the lines emerging at high deposition temperature, their presence in all emission groups suggests that the emission takes place from the $^4F_{3/2}$ energy level of a Nd^{3+} ion. A different lattice site could explain the slightly different emission pattern, but the absence of Nd^{3+} absorption levels in the PLE spectra of these lines must be taken into account. Two types of transfer are possible from the host, leading to Nd^{3+} emission. Either one 4f electron of a Nd^{3+} ion is excited by non-radiative energy transfer to a higher level or one electron from the conduction band of the host is trapped by Nd^{4+}, which temporarily reduces to the 3+ state. The NdO_2 crystal is not stable under ambient conditions[21] and therefore a pure 4+ state is unlikely to be present. However, some Nd^{3+} ions could lose some more charge (*e.g.* to interstitial oxygen) to form an intermediate state. Ions in such a state could be temporarily reduced to the 3+ state by trapping one electron from the host.

Since the presence of Nd^{4+} requires a different crystal field, the slightly different emission pattern observed could be explained. In addition, these ions would have only one 4f electron under normal conditions, which means that the excitation spectrum is totally different. All excited states of Nd^{4+} are highly energetic,[22] which means that these ions can only be excited by far UV light illumination.

However, the observed signals could also be explained by a second Nd site whose valence state is 3+. If the number of sites is small, but the transfer mechanism is particularly efficient, both the absence of strong direct excitation and the high emission intensity under indirect excitation can be explained.

The NEXAFS measurement of the ZnO:Nd thin films was performed to investigate the valence state of Nd (see Fig. S3 in the ESI†). The data indicate that the greatest part of the Nd ions is in the 3+ state. However, if there was a small amount of ions in a different oxidation state, say one to one hundred Nd ions, even this sophisticated technique would not detect it. In addition, the already low concentration of Nd in the film allows only detection in TEY mode, which sounds only the first few nanometers of the film.

In conclusion, both explanations suggest the existence of a small number of active sites with high transfer efficiency from the host. Unfortunately, such small concentrations push many techniques to their physical limits, which makes the interpretation of the optical data quite difficult.

In Fig. 8, the information obtained by the study of PL and PLE spectra is summarized. The direct excitation peaks and emission peaks of Nd^{3+} which could be attributed to the highest confidence are indicated by the arrows. Due to the complex nature of the absorption and emission spectra, it was not possible to reconstruct a complete energy level diagram of Nd^{3+} in ZnO. However, valuable information has been obtained concerning the origin of the observed transitions.

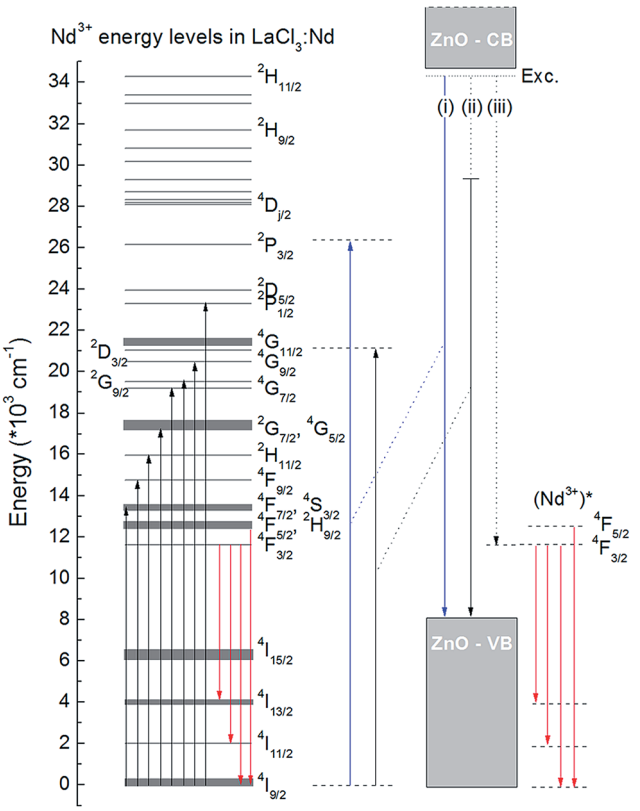

Fig. 8 Observed radiative transitions of Nd^{3+} in ZnO and possible energy transfer mechanisms from the host. The energy levels of Nd^{3+} in $LaCl_3$ are taken from ref. 18.

In particular, the three transfer mechanisms which might be responsible for the energy transfer from the host are shown on the right side of Fig. 8. Mechanism (i) represents the ideal case when band-to-band or exciton recombination transfers all the energy to one 4f electron of Nd^{3+}. In mechanism (ii), the energy transfer occurs through some localized defect states within the band gap. Mechanism (iii) accounts for the emerging features observed at high deposition temperature and involves electron trapping by Nd^{4+} ions. In particular, the case when the electron is trapped by the lowest excited state in the gap. Although the exact position of Nd levels with respect to the ZnO bands has never been measured experimentally, theoretical calculations indicate that the fundamental state of Nd^{3+} is situated at about 1 eV below the top of the valence band.[23] If this was the case, then the lowest level in the gap would be exactly the level from which the emission takes place. If on the other hand the explanation to the new patterns is the existence of several Nd^{3+} active sites, then several (ii)-type processes occur.

One last consideration should be done, regarding the variation of the band gap with the deposition temperature. Indeed, a variation of the gap could change the resonance condition between the levels of the host and the RE and explain a strong increase in the PL. However, since the PL only occurs from the $^4F_{3/2}$ and $^4F_{5/2}$ levels, the same emission pattern would be expected. The change in the relative emission intensity of the peaks excludes this hypothesis and favors the explanation based on several active sites of Nd.

Conclusions

High quality Nd-doped ZnO thin films have been obtained by means of the RF sputtering technique. Nd atoms are uniformly distributed along the growth direction and the presence of optically active Nd ions has been confirmed by PL measurements.

Despite the low RE quantity in these thin ZnO films, intense PL signals have been collected, indicating efficient IR emission of Nd^{3+} in ZnO. No evidence of down conversion was observed in the frame of the investigated parameters. However, Nd-doped ZnO can find applications as an efficient downshifter.

Due to the very rich nature of the Nd^{3+} energy level structure, interpretation of the luminescence signals is not straightforward. If the structural information does not offer a clue to the problem, the combination of PL and PLE analysis performed on a wide spectral range and down to cryogenic temperatures allowed identification of several transitions related to Nd ions in ZnO and valuable information has been obtained about their origin.

Three emission groups have been attributed to the $^4F_{3/2} \rightarrow {}^4I_J$ emission of Nd^{3+} ions and one to the $^4F_{5/2} \rightarrow {}^4I_{9/2}$ emission. A closer look at the emission spectra showed that several additional emission lines are present, compared to those expected from the spectroscopic level multiplicity. The intensity of some of these lines strongly increase for deposition temperatures above 400 °C. These lines have been attributed to a different active site for Nd and several transfer mechanisms have been proposed. The fact that these intense lines emerge from all

emission groups and that no absorption from Nd^{3+} is visible in their excitation spectra suggests two possible explanations. Either this emission involves Nd^{3+} ions that are slightly more oxidized, or a small amount of Nd^{3+}ions that are in a second active site and for which the transfer from the host is particularly efficient. The small concentrations involved challenge the most sensitive analysis techniques and prevent us from selecting one single transfer mechanism.

Some additional features, such as the emission peaks at 916 nm and at 895 nm, are more difficult to explain. The presence of a third active site and of an additional transition from a higher level of Nd^{3+} might be the origin of these peaks.

Acknowledgements

Element-specific near edge X-ray absorption fine structure (NEXAFS) spectroscopy experiments were performed at the Canadian Light Source, which is funded by the Canada Foundation for Innovation, the Natural Sciences and Engineering Research Council of Canada, the National Research Council Canada, the Canadian Institutes of Health Research, the Government of Saskatchewan, Western Economic Diversification Canada, and the University of Saskatchewan. The authors would like to thank G. Schmerber for performing the XRD measurements and M. Ziegler for helping with the luminescence setup.

References

1 A. J. Steckl, J. C. Heikenfeld, L. Dong-Seon, M. J. Garter, C. C. Baker, W. Yongqiang and R. Jones, *IEEE J. Sel. Top. Quantum Electron.*, 2002, **8**, 749–766.
2 X. Zeng, J. Yuan and L. Zhang, *J. Phys. Chem. C*, 2008, **112**, 3503–3508.
3 L. Li, C. K. Tsung, Z. Yang, G. D. Stucky, L. D. Sun, J. F. Wang and C. H. Yan, *Adv. Mater.*, 2008, **20**, 903–908.
4 B. S. Richards, *Sol. Energy Mater. Sol. Cells*, 2006, **90**, 2329–2337.
5 D. Chen, Y. Wang and M. Hong, *Nano Energy*, 2012, **1**, 73–90.
6 I. Soumahoro, G. Schmerber, A. Douayar, S. Colis, M. Abd-Lefdil, N. Hassanain, A. Berrada, D. Muller, A. Slaoui, H. Rinnert and A. Dinia, *J. Appl. Phys.*, 2011, **109**, 033708.
7 M. Balestrieri, G. Ferblantier, S. Colis, G. Schmerber, C. Ulhaq-Bouillet, D. Muller, A. Slaoui and A. Dinia, *Sol. Energy Mater. Sol. Cells*, 2013, **117**, 363–371.
8 H. Rinnert, P. Miska, M. Vergnat, G. Schmerber, S. Colis, A. Dinia, D. Muller, G. Ferblantier and A. Slaoui, *Appl. Phys. Lett.*, 2012, **100**, 101908.
9 R. Pandiyan, R. Bartali, V. Micheli, G. Gottardi, I. Luciu, D. Ristic, G. A. Goget, M. Ferrari and N. Laidani, *Energy Procedia*, 2011, **10**, 167–171.
10 D. C. Look, *Mater. Sci. Eng., B*, 2001, **80**, 383–387.
11 G. Gottardi, R. Pandiyan, V. Micheli, G. Pepponi, S. Gennaro, R. Bartali and N. Laidani, *Mater. Sci. Eng., B*, 2013, **178**, 609–616.
12 C. Davesnne, A. Ziani, C. Labbé, P. Marie, C. Frilay and X. Portier, *Thin Solid Films*, 2014, **553**, 33–37.
13 J. Petersen, C. Brimont, M. Gallart, G. Schmerber, P. Gilliot, C. Ulhaq-Bouillet, J.-L. Rehspringer, S. Colis, C. Becker, A. Slaoui and A. Dinia, *J. Appl. Phys.*, 2010, **107**, 123522.
14 F. Xian and X. Li, *Opt. Laser Technol.*, 2013, **45**, 508–512.
15 A. Douayar, M. Abd-Lefdil, K. Nouneh, P. Prieto, R. Diaz, A. O. Fedorchuk and I. V. Kityk, *Appl. Phys. B*, 2013, **110**, 419–423.
16 A. Douayar, P. Prieto, G. Schmerber, K. Nouneh, R. Diaz, I. Chaki, S. Colis, A. El Fakir, N. Hassanain, A. Belayachi, Z. Sekkat, A. Slaoui, A. Dinia and M. Abd-Lefdil, *Eur. Phys. J.: Appl. Phys.*, 2013, **61**, 10304.
17 Y. Liu, W. Luo, R. Li and X. Chen, *J. Nanosci. Nanotechnol.*, 2010, **10**, 1871–1876.
18 G. H. Dieke, *Spectra and Energy Levels of Rare Earth Ions in Crystals*, Interscience Publishers, New York, 1968.
19 C. Klingshirn, M. Grundmann, A. Hoffmann, B. Meyer and A. Waag, *Phys. J.*, 2006, **5**, 33–38.
20 T. Fix, H. Rinnert, M. G. Blamire, A. Slaoui and J. L. MacManus-Driscoll, *Sol. Energy Mater. Sol. Cells*, 2012, **102**, 71–74.
21 L. Petit, A. Svane, Z. Szotek and W. Temmerman, in *Rare Earth Oxide Thin Films*, ed. M. Fanciulli and G. Scarel, Springer, Berlin Heidelberg, 2007, vol. 106, ch. 19, 331–343.
22 A. Meftah, J.-F. Wyart, J. Sinzelle, W.-Ü. L. Tchang-Brillet, N. Champion, N. Spector and J. Sugar, *Phys. Scr.*, 2008, **77**, 055302.
23 P. Dorenbos and E. van der Kolk, *Proc. SPIE 6473, Gallium Nitride Materials and Devices II*, San José, California, 2007, 647313.